Science Advances

AAAS

advances.sciencemag.org/cgi/content/full/2/10/e1600964/DC1

Supplementary Materials for

Constructing 3D heterogeneous hydrogels from electrically manipulated prepolymer droplets and crosslinked microgels

Min-Yu Chiang, Yao-Wen Hsu, Hsin-Yi Hsieh, San-Yuan Chen, Shih-Kang Fan

Published 26 October 2016, *Sci. Adv.* **2**, e1600964 (2016)
DOI: 10.1126/sciadv.1600964

The PDF file includes:

Other Supplementary Material for this manuscript includes the following:
(available at advances.sciencemag.org/cgi/content/full/2/10/e1600964/DC1)

- movie S7 (.mpg format). Manipulation and crosslinking of microgels with cells (Fig. 4I).

Supplementary Materials

Electrowetting (EWOD)

Electrowetting modulates the apparent contact angle of a conductive liquid droplet on a solid electrode coated with dielectric and hydrophobic layers on application of a voltage. The variation of contact angle from θ_0 to $\theta(V)$ on applying voltage V_{EWOD} across a dielectric layer is expressed with the Lippmann-Young equation

$$\cos\theta(V) = \cos\theta_0 + \frac{\varepsilon_0 \varepsilon_D}{2\gamma_{LG} t} {V_{EWOD}}^2 \quad (1)$$

in which ε_0 (8.85×10^{-12} F/m) denotes the permittivity of vacuum, ε_D the relative permittivity of the dielectric layer of thickness t, γ_{LG} the liquid-gas interfacial tension and V_{EWOD} the voltage drop across the dielectric layer. Electrowetting is generally evaluated with a sessile-drop method as shown in the insets of Fig. 1B. Unpatterned ITO-coated glass plates were coated with SU-8 (thickness 1.7 μm) and Teflon (thickness 55 nm). DI water, water/PEGDA mixture (20 and 50% v/v), and pristine PEGDA droplets (1.5 μL) were dispensed on to the Teflon surface. A tungsten wire (diameter 70 μm) was inserted into the droplet. The contact angles were measured on application of 1-kHz square-wave AC signals at 0-140 V_{RMS}.

Based on the Laplace-Young equation, the contact angle variation develops pressure differences between the two ends of the droplet (width W) and causes a pumping force of the droplet (fig. S1A)

$$F_{EWOD} = \frac{\varepsilon_0 \varepsilon_D W}{2t} {V_{EWOD}}^2 \quad (2)$$

Dielectrophoresis on liquids (LDEP)

Dielectrophoresis supplies surface forces to draw bulk liquids, including dielectric liquids, of greater relative permittivity into a region of strong electric field of smaller relative permittivity (e.g., air). As illustrated in fig. S1A, on applying voltage V_{LDEP} between parallel electrodes (spacing d) and neglecting the voltage in the dielectric layer, a dielectric oil droplet is attracted toward the region of strong electric field with a dielectrophoretic force F_{LDEP}

$$F_{LDEP} = \frac{\varepsilon_0(\varepsilon_{Oil}-\varepsilon_{Air})W}{2d} {V_{LDEP}}^2 \quad (3)$$

in which ε_{Oil} and ε_{Air} are the relative permittivities of oil and air, respectively.

The velocity of dielectric PEGDA prepolymer droplets driven by dielectrophoresis using a 1-kHz square-wave AC signal at varied applied voltages is shown in Fig. 1C. The tested pristine PEGDA droplet (volume 0.1 μL, diameter 1 mm, height 100 μm) was driven back and forth along five driving electrodes (1 mm × 1 mm) at tested voltages to examine the maximum driving velocity. At a given voltage, the minimum switching time *T* achieving the successful droplet movement was recorded, and the velocity (1 mm/*T*) was calculated, averaged from three experiments, and is plotted in Fig. 1C.

Dielectrophoresis on particles (DEP)

As shown in the right droplet of fig. S1B, when the electric field within a prepolymer solution or water droplet is non-uniform, particles are polarized and actuated by dielectrophoresis. The dielectrophoretic force, F_{DEP}, exerted on a spherical particle of radius *r* is described as

$$F_{DEP} = 2\pi r^3 \varepsilon_L \mathrm{Re}\left(\frac{{\varepsilon_P}^* - {\varepsilon_L}^*}{{\varepsilon_P}^* + 2{\varepsilon_L}^*}\right) \nabla E^2 \quad (4)$$

in which *E* denotes electric field, ε_P* and ε_L* the complex permittivities of the manipulated particles and of the suspension liquid, respectively, which depend on frequency, expressed as

$${\varepsilon_{P,L}}^* = \varepsilon_0 \varepsilon_{P,L} - j\frac{\sigma_{P,L}}{2\pi f} \quad (5)$$

in which $\varepsilon_{P,L}$ is the relative permittivity and $\sigma_{P,L}$ the conductivity of the particle or the suspension liquid; *f* is the frequency of the electric field. When F_{DEP} is greater than zero, particles are attracted toward a region of large field strength, which is referred to as positive dielectrophoresis. On the contrary, negative dielectrophoresis repels particles from regions of large field strength. As shown in Fig. 3, H to K, movie S5, and Fig. 4, A to D, the particles were driven in PEGDA by negative dielectrophoresis when applying a 100-V_{RMS} and 1-kHz square-wave AC signal on the patterned driving electrodes. Negative dielectrophoresis on patterned electrode 6 reorganized NIH/3T3 fibroblasts in GelMA (fig. S1F). With

patterned electrode 2, fibroblasts in GelMA were reorganized with positive and negative dielectrophoresis as shown in Fig. 4I and fig. S1G, respectively.

Dielectrophoresis of crosslinked microgels (SDEP)

Crosslinked microgels are driven on the electromicrofluidic platform between two plates, similar as moving a dielectric slab between electrodes. F_{SDEP} exerting on crosslinked microgels (fig. S1B) can be simplified when neglecting the voltage drop in the dielectric layer as

$$F_{SDEP} = -\frac{\varepsilon_0(\varepsilon_{Slab}-\varepsilon_{Medium})W}{2d}{V_{SDEP}}^2 \quad (6)$$

in which ε_{Slab} and ε_{Medium} are the relative permittivities of the crosslinked microgel and the surrounding medium, respectively. When the medium (e.g., prepolymer solution or water) possesses a greater relative permittivity than the slab, the crosslinked microgel is driven away from the region of strong field.

As listed in fig. S1J, the crosslinked PEGDA microgels were harvested and then driven in water (Fig. 2, A to C and movie S2) with a 20-V_{RMS} and 100-kHz square-wave AC signal and in photocrosslinkable PEGDA prepolymer solution (Fig. 3, B to G and movie S4) with a 115-$V_{RMS}$and 100-Hz square-wave AC signal.

Supplementary Figures

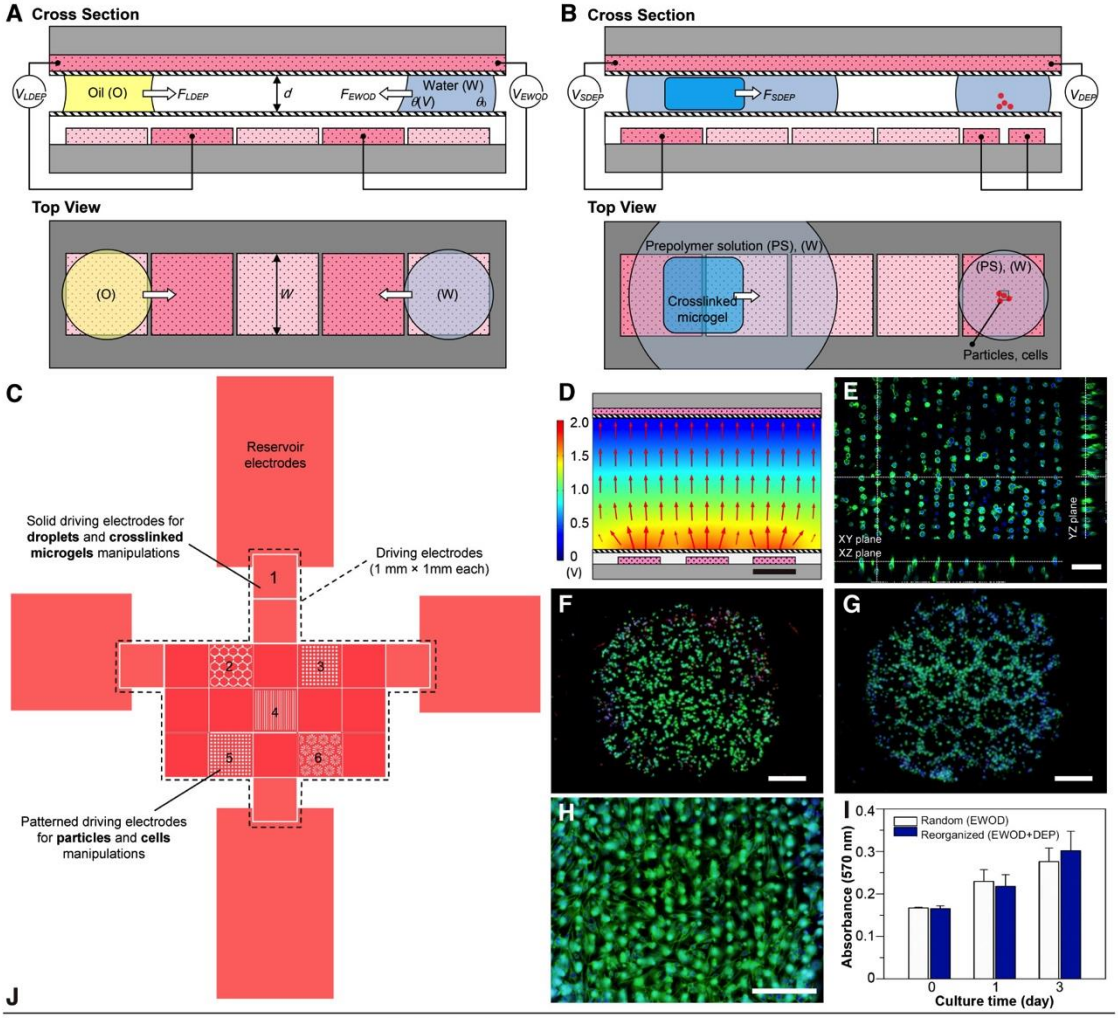

Manipulated objects	Scale	Phase	Environment (height (μm))	Applied signal	Major mechanism	Demonstrations
Water sessile drop	mm	Liquid	Air	1 kHz	Electrowetting	Fig. 1B
PEGDA droplet	mm	Liquid	Air (100)	100 V_{RMS}, 1 kHz	Dielectrophoresis	Fig. 1C-K, 2D-E, 3A, H-I, 4A-D, Movie S1, S3, S5
GelMA droplet	mm	Liquid	Oil shell in air (200)	30 V_{RMS}, 100 kHz	Electrowetting	Fig. 4G, I, Movie S7
Matrigel droplet	mm	Liquid	Oil shell in air (100)	40 V_{RMS}, 100 kHz	Electrowetting	Fig. 3A
Polyacrylamide droplet	mm	Liquid	Oil shell in air (100)	40 V_{RMS}, 100 kHz	Electrowetting	Fig. 3A
PEGDA microgel	mm	Solid	Water (300)	20 V_{RMS}, 100 kHz	Dielectrophoresis	Fig. 2A-C, Movie S2
PEGDA microgel	mm	Solid	Liquid PEGDA (300)	115 V_{RMS}, 100 Hz	Dielectrophoresis	Fig. 3B-G, Movie S4
Particle	μm	Solid	Liquid PEGDA (100)	100 V_{RMS}, 1 kHz	Dielectrophoresis	Fig. 3I, 4A-D, Movie S5
Fibroblasts	μm	Mixed	Liquid GelMA (200)	2.2 V_{RMS}, 1 MHz	Dielectrophoresis	Fig. 4I, Movie S7

fig. S1. Configuration and manipulations on an electromicrofluidic platform. (**A**) Conductive (water) and dielectric (oil) droplets are driven with electrowetting and dielectrophoresis, respectively, towards the energized driving electrode. (**B**) Particles (μm) and crosslinked microgels (mm) are driven in a

prepolymer solution or aqueous environment with dielectrophoresis and a non-uniform electric field, and, in this example, expelled from the regions of strong field. (**C**) Design of the driving and reservoir electrodes on the bottom plate. Solid and patterned driving electrodes are designed for various manipulations. (**D**) Simulated electric potential and field across water (conductivity 5.5×10^{-8} S/cm, relative permittivity 80, thickness 100 μm) between the plates when DEP signal was applied (1 MHz and 2.2 V_{RMS}) using electrode 4 in (C). (**E**) Fluorescence confocal microscopy image of a GelMA microgel (thickness 100 μm) with NIH/3T3 fibroblasts reorganized with electrode 4 in (C) and stained with Alexa Fluor® 488 phalloidin and DAPI after 12 h in culture. (**F** and **G**) GelMA microgels as crosslinked with encapsulated NIH/3T3 fibroblasts reorganized with negative dielectrophoresis using electrode 6 and 2 in (C) to form lobule-like cell clusters (F) and honeycomb-like cell networks (G), respectively, and stained with Hoechst 33342 (nuclei, blue), calcein AM (live cells, green), and EthD-1 (dead cells, red). (**H**) Pseudopodia extension observation in a GelMA microgel with NIH/3T3 reorganized with electrode 4 in (C) and stained with Alexa Fluor® 488 phalloidin and DAPI on day 3 in culture. (**I**) MTT assay of GelMA microgels with random and reorganized cells at day 0, 1, and 3 in culture; ODs at wavelength 570 nm were 0.167 and 0.165 at day 0, 0.230 and 0.218 at day 1, and 0.302 and 0.277 at day 3 for random and reorganized cells, respectively. (**J**) Manipulations on the electromicrofluidic platform. Scale bar: (D) 30 μm; (E) 100 μm; (F to H) 200 μm.

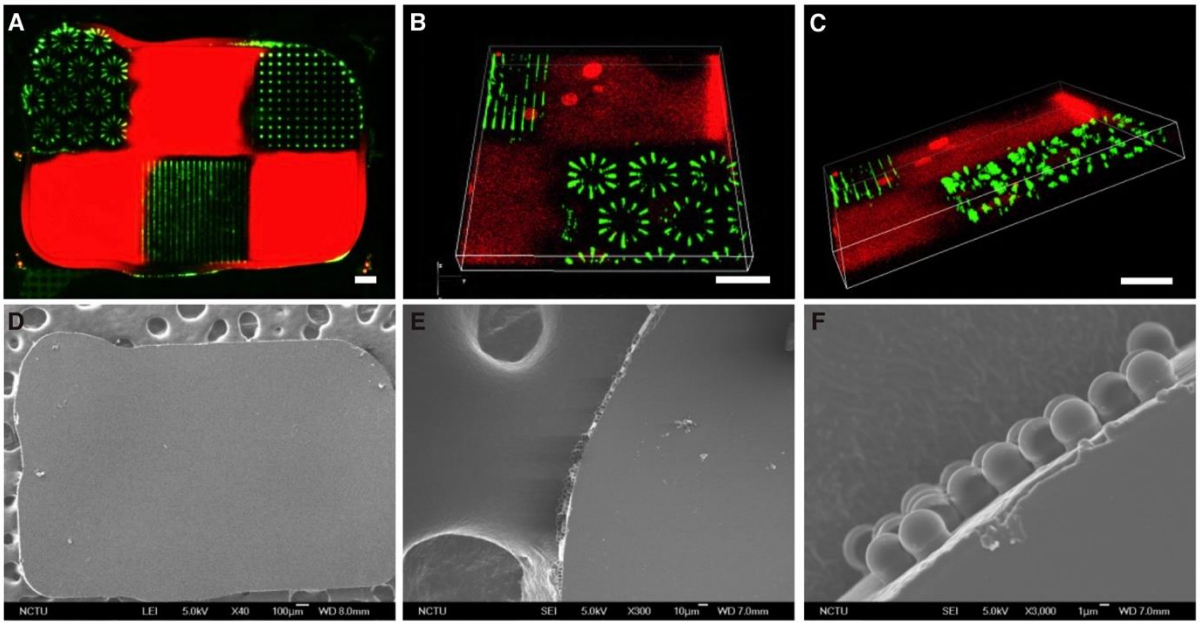

fig. S2. Visualization of a heterogeneous architecture with a fluorescence microscope, a fluorescence confocal microscope, and an SEM. (**A**) Fluorescence microscopy image of the assembled heterogeneous architecture containing 3 × 2 microgels with dye and particles. (**B** and **C**) Angled views of the architecture examined with a confocal microscope showing a seamless interface between dye and particle microgels. (**D** to **F**) SEM observation at varied magnifications showing the smooth and flat surface topography and particles adhered on the side surface. Scale bar: (A to C) 200 μm.

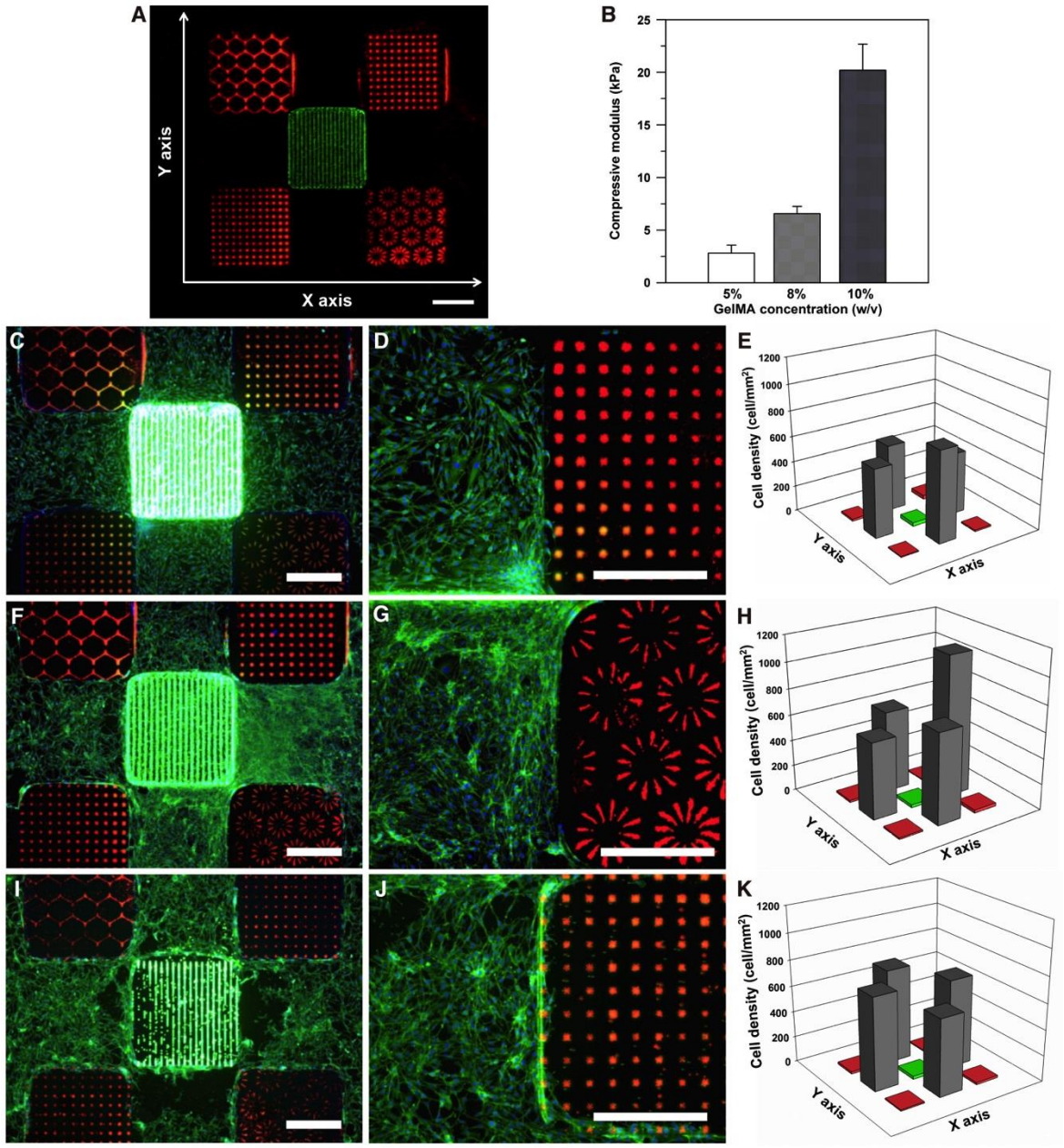

fig. S3. NIH/3T3 fibroblast culture on heterogeneous architecture composed of PEGDA and GelMA. (**A**) Fluorescence microscopy image of heterogeneous architecture before cell seeding and culture; PEGDA contained reorganized fluorescent green and red particles, whereas GelMA, shown black, did not. (**B**) Compressive moduli (2.8, 6.6, and 20.2 kPa) of GelMA at various concentrations (5, 8, and 10%, respectively). (**C** to **K**) At 48 h in culture, the fluorescence microscopy images and the cell densities of the architectures consisting of PEGDA and GelMA at 5% (C to E), 8% (F to H), and 10%

w/v (I to K) show that cells mainly adhered on 5, 8, and 10% GelMA at the cell concentrations of 567.2, 751.9, and 680.6 cells/mm^2, respectively. Scale bar: 500 μm.

movie S1. Manipulation and crosslinking of liquid microgels (Fig. 1J). Preparation of microgels (volume 0.1 μL) with configurable encoding colors from reservoirs accommodating PEGDA with R (right), G (upper) and B (left) fluorescent dyes.

movie S2. Postcrosslinking assembly of microgels (Fig. 2, A to C). Postcrosslinking assembly and stacking of crosslinked PEGDA microgels (1 mm × 1 mm × 100 μm) in an aqueous environment.

movie S3. Precrosslinking assembly of microgels (Fig. 2, D and E). Precrosslinking assembly of nine PEGDA droplets with varied dyes to form a heterogeneous architecture (3 mm × 3 mm × 100 μm).

movie S4. Postcrosslinking assembly of microgels with particles (Fig. 3, B to G). Postcrosslinking assembly and stacking of crosslinked PEGDA microgels, containing random and reorganized fluorescent red particles, in liquid PEGDA prepolymer solution observed with fluorescence and bright-field microscope.

movie S5. Precrosslinking assembly of microgels with particles (Fig. 3, H and I). Precrosslinking assembly of nine PEGDA droplets with dye and reorganized particles to form a heterogeneous architecture (3 mm × 3 mm × 100 μm).

movie S6. Beating of patterned cardiomyocytes at 24 and 48 hours in culture (Fig. 4F). Observation of patterned neonatal mouse cardiomyocytes beating on a heterogeneous architecture composed of PEGDA and GelMA at 24 and 48 hours in culture.

movie S7. Manipulation and crosslinking of microgels with cells (Fig. 4 I). Aliquoting of GelMA (5% w/v) prepolymer droplet and reorganizing NIH/3T3 fibroblasts for 3D cell culture.